T H E U N I V E R S I T Y O F M I C H I G A N

SCHOOL OF PUBLIC HEALTH
Department of Industrial Health

Final Report

DEVELOPMENT OF A CONTINUOUS AEROSOL MONITOR

Charles E. Billings

ORA Project 08850

under contract with:

AMERICAN IRON AND STEEL INSTITUTE
TECHNICAL COMMITTEE ON AIR AND WATER QUALITY
NEW YORK, NEW YORK

administered through:

OFFICE OF RESEARCH ADMINISTRATION ANN ARBOR

September 1967

engn

UMR0397

TABLE OF CONTENTS

LIST OF TABLES

LIST OF FIGURES

ABSTRACT

This report describes results of research on the accumulation of 1.305 μ polystyrene latex spheres on Fiberglas filters. Initial change in pressure drop was linear with time over a 1 hr period as predicted theoretically with an average slope of 0.70 in. gauge oil/hr, while filtering 1600 p/cm (45 mppcf, 0.9 grains/1000 cu ft) at a constant velocity of 40.2 cm/sec. Methods are described for using this linear behavior of filter pressure drop with time in an aerosol monitor for continuous automatic determination of stack, duct, dust collector, and ambient dust concentrations. Feasibility and cost of various transducer and data treatment systems are discussed.

I. INTRODUCTION

This report describes research on a continuous aerosol particle monitor for the American Iron and Steel Institute, Technical Committee on Air and Water Quality, during the period May 1, 1967 to August 31, 1967. The objective of this project is to develop a system to sample particulate matter from an atmosphere. It is proposed to deposit this material on a porous substrate and measure the amount of the deposit in terms of mass or number concentration by means of the change in flow resistance caused by the accumulated particles. Applications of this system include routine quantitative analysis (monitoring) of process or effluent gas streams for particulate components such as dusts, fumes, mists, or tar droplets (e.g., blast furnace gas, natural gas), mill, furnace or motor room air quality, dust collector performance (by sampling and recording the ratio of outlet to inlet dust samples) and urban particulate air quality.

During the period covered by this report, an aerosol generating and sampling system has been constructed to study the effects of accumulating particulate materials on fibrous filters, and preliminary investigations have been undertaken to evaluate the feasibility of various pressure transducers and associated electronic signal analysis systems. Two graduate students of The University of Michigan have been actively engaged in the research described in this report: Mr. John Johnson (M.S., Electrical Engineering, currently working toward the Ph.D. degree), and Mr. Robert Fidelman (B.S., Naval Architecture, currently working toward the M.S. degree). They have performed much of the ex-

perimental work described below, and have prepared parts of this report. Their help is gratefully acknowledged.

II. EFFECTS OF PARTICLE ACCUMULATION ON FILTER PRESSURE DROP

A. THEORY

A standard filter paper tape sampler has been proposed to collect particles for the initial development of the continuous aerosol monitor. This consists of a solenoid operated sampling head, a continuous filter tape directed through the head, a vacuum source to provide sample air flow into the head and through the tape, a sample air flow meter and regulator, and a programmed switch and valve system to order the sequence of sample and advance tape in a piece-wise continuous manner.

As solid or liquid particulate matter deposits on the tape, it produces an increase in the air flow resistance. If the tape completely removes the particulate matter, the increment in resistance is a linear function of the quantity of material deposited.

Consider a filter of packing density $\rho_b (gm/cm^3)$ composed of fibrous material of density $\rho_m (gm/cm^3)$. The fraction of fiber solids in the filter is defined as:

$$\alpha = \rho_b/\rho_m \, . \tag{1}$$

The length of the fiber per unit volume is

$$\ell = \alpha/\pi a^2 \tag{2}$$

where a is the fiber radius. Let F_D be the total drag force per unit length of fiber exposed to an aerosol stream of velocity U_o, containing particles of radius

a_p. As particles accumulate on the fiber and on previously deposited particles, the drag force will increase. Assume that the total drag force at any instant of operation can be expressed by two independent terms, such as:

$$F_D = R_D(0) + (S_p \mu U_o a_p) 2aZ \tag{3}$$

where $R_D(0)$ represents the initial drag force on the fiber at the start of filtration, $2aZ$ is the local deposition per unit length of fiber, Z is the number of particles deposited per unit projected area of fiber (p/cm^2 of fiber), and $(S_p \mu U_o a_p)$ represents the drag per particle on the fiber (for a free particle, the dimensionless particle resistance coefficient S_p would be 6π as given by Stokes, but for the deposited particle it is unknown and found by experiment).

The drag force per unit volume of mat can be set equal to the pressure gradient:

$$\ell F_D = \frac{dp}{dx} \tag{4}$$

where ℓ is the length of fiber per unit volume given by Eq. (2), and p the local pressure. By substituting Eq. (3) and integrating from $p = p_o$ at $x = 0$ (entrance to the filter) to $p = p_L$ at $x = L$ (exit from the filter) the pressure drop across the filter mat becomes:

$$\frac{1}{L} \int_{p_o}^{p_L} dp = \frac{\Delta p}{L} = \ell F_D(0) + \frac{2a\ell}{L} (S_p \mu U_o a_p) \int_o^L Z dx. \tag{5}$$

The increment in filter resistance arising from the deposition of particles will be:

$$\frac{\Delta p}{L} - \ell F_D(0) = \frac{\delta \Delta p}{L} = \frac{2a\ell}{L} \cdot \frac{\pi a}{2\alpha} \cdot (S_p \mu U_o a_p) U_o N_o t \ , \tag{6}$$

where accumulation (particles per cm^2 of filter face area) has been expressed as:

$$A = U_o N_o t = \frac{2\alpha}{\pi a} \int_o^L Z dx \ . \qquad (7)$$

For a filter which removes all particles:

$$\delta \Delta p = (S_p \mu U_o a_p) U_o N_o t \ . \qquad (8)$$

Equation (8) indicates that the resistance rise per unit of filter depth produced by the deposit ($\delta \Delta p/L$) should be proportional to the drag per particle ($S_p \mu U_o a_p$) and the particle concentration in the bed (A/L). The dimensionless resistance coefficient S_p has been shown to be a function of fiber fraction[1]:

$$S_p = 33\alpha \qquad (9)$$

over the range $0.007 \leq \alpha \leq 0.035$. For a given filter material, S_p should be relatively constant since α will not vary widely for filters of 100% efficiency.

In an aerosol whose particle size spectrum remains constant during the sampling period, the time derivative, or increment over a fixed interval, of the increase in resistance is proportional to the number concentration (and mass concentration) of the particles. By measuring and recording the sum of the resistance of the filter and deposited particles, subtracting the constant initial resistance and forming the increment ($\delta \Delta p/\Delta t$) an output can be obtained which is proportional to the deposit density in the initial stages of deposition when the particles are effectively far apart.

The time interval required for a measurable pressure increment depends upon the aerosol flux, $U_o N_o$. Filtering velocity (U_o) can be increased or decreased

as required by the concentration levels (N_o) in the sampled atmosphere. The change in resistance ($\delta\Delta p$) is proportional to the square of the flow velocity, so the proposed method is particularly useful for low concentrations where, for example, a doubling of the sampling velocity will produce four times the increment in resistance during a given time interval. This method should apply to any particulate material, liquid or solid, depending only the particle size, and not on chemical or atomic properties of the matter. The sensitivity (detectable particle concentration level) is discussed below in the experimental section.

B. EXPERIMENTS

1. Apparatus

The theory discussed above predicts that the initial stages of accumulation of particles on a fibrous filter of 100% efficiency will produce an increase in pressure drop which is a linear function of time, at constant filtration velocity and particle concentration. Several experiments were conducted to evaluate the pressure drop response of filter papers during filtration of solid and liquid particles. Test apparatus is shown in Fig. 1 and consists of an aerosol generator, an aerosol tunnel and a flowmeter system. The tunnel test filter holder is shown in Figs. 2 and 3.

The test section consisted of two pieces of 1-1/2 in. diam hard-drawn copper tubing, each 3 in. long. A modified brass union was used to hold test mat and and fiber specimens, as shown in Fig. 2. Static pressure holes (0.040 in. diam) and pressure taps were provided to measure pressure differential across the test

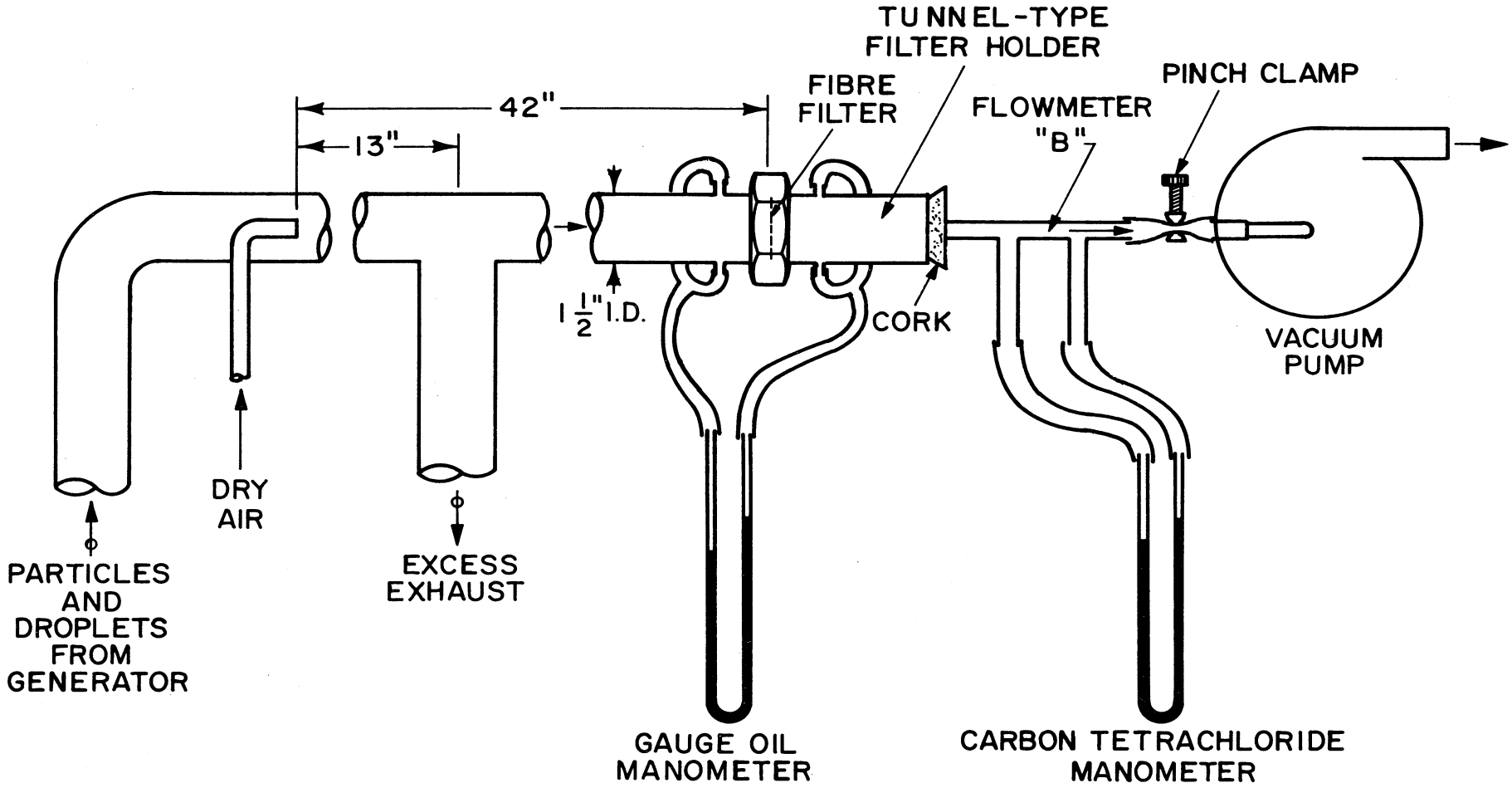

Fig. 1. Aerosol tunnel.

LEGEND FOR FIGURES 2 AND 3

A. Test Section Inlet

B. Test Section Union Nut

C. Static Pressure Tap

D. Test Mat Holder and Test Section Outlet

E. Neoprene "O"-Ring

F. Aluminum Spacer Ring
48 mm O.D.x39 mm I.D.x2 mm Thick

G. Aluminum Foil Gasket (48x40)

H. Filter Mat Retaining Screen and Spacer
48 mm O.D.x39 mm I.D.x1 mm Thick with Soldered Screen (16 mesh x 0.010 in wire) and Reinforcing Cross

I. Glass Fiber Paper Gasket
48 mm O.D.x40 mm I.D.x1 mm Thick

J. Filter Thickness Spacer
48 mm O.D.x46 mm I.D.x1 mm or 2 mm Thick

K. Typical Test Filter Mat

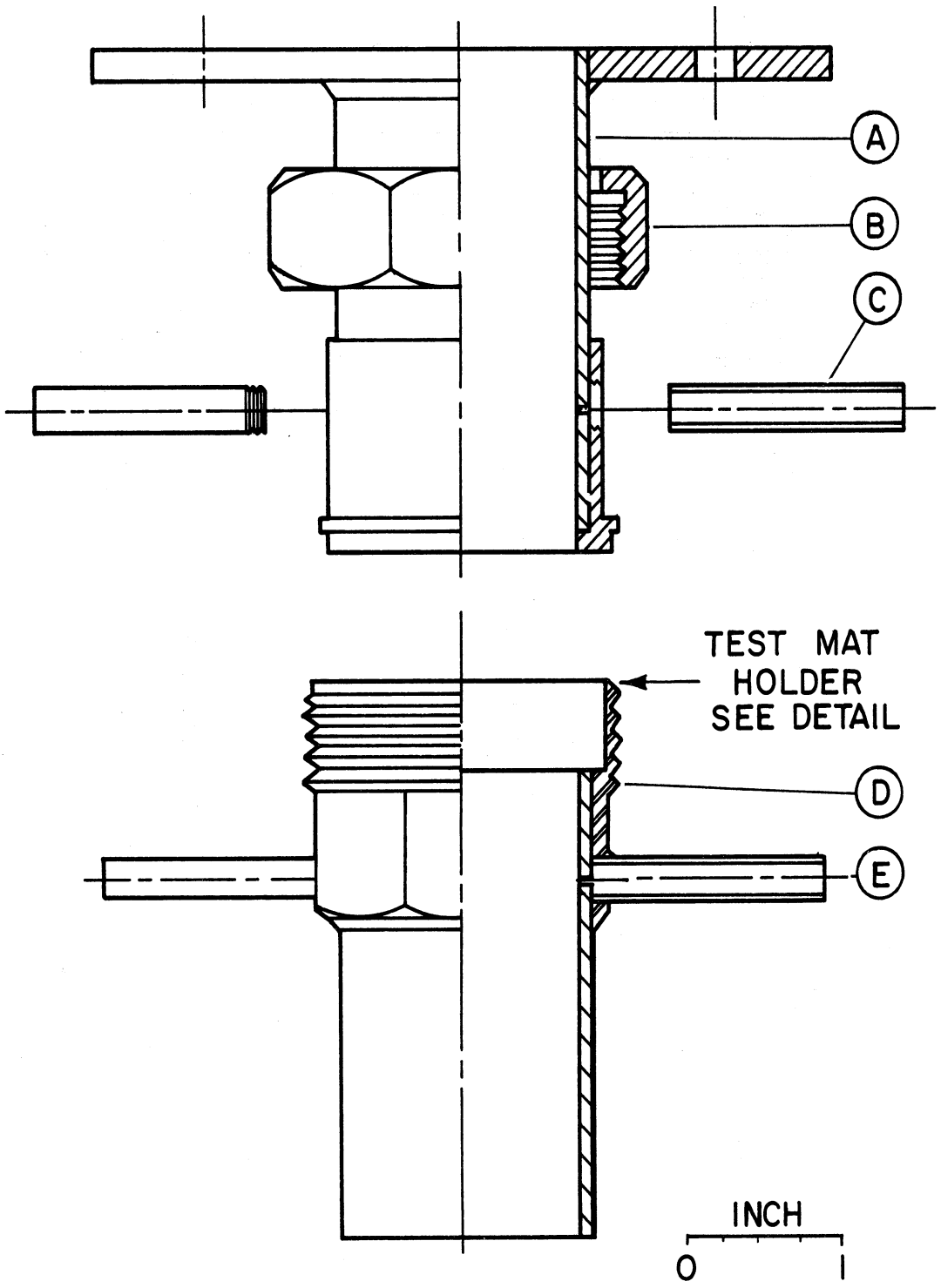

Fig. 2. Aerosol tunnel test section.

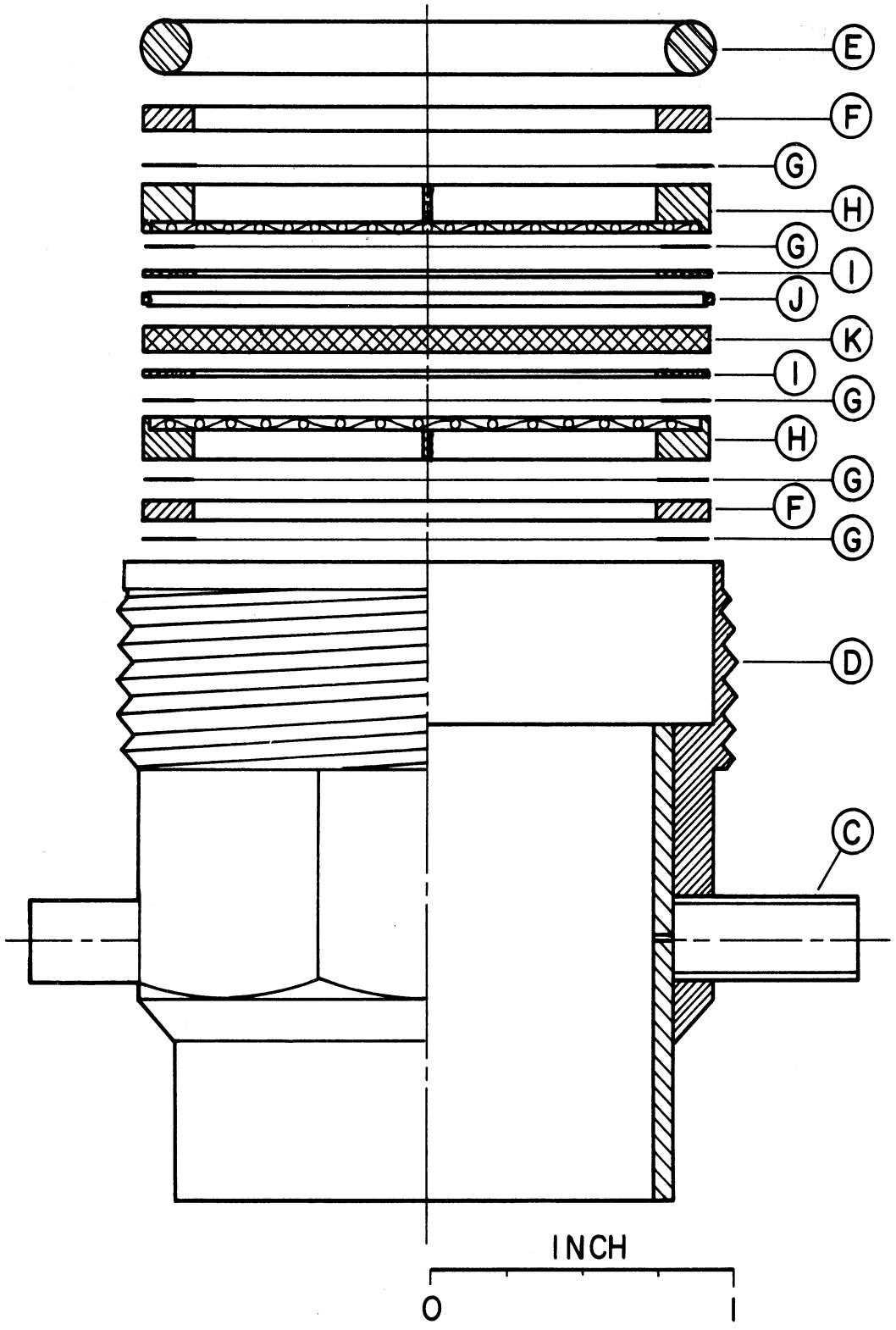

Fig. 3. Test filter holder detail.

section screens and filters.

Filter mats were held in the test position by the two halves of the union and the union nut. They were retained between two screens supported by rings and a stiffening cross as shown in detail in Fig. 3. Distance between the two screens was set by a spacer. Two gaskets were made from all-glass filter paper and placed on either face of the test mat to reduce edge leakage or aerosol by-passing. Aluminum foil gaskets of the same diameters as the glass paper gaskets were placed between them and the screen surface to promote compression.

Additional aluminum ring spacers and foil and rubber gaskets were used as required to fill the test section holder, and prevent leakage. A neoprene "O" ring was used between the top aluminum ring spacer and the companion flange of the upper half of the test section union as shown in Fig. 3. The whole assembly was placed up on the mating flange on the aerosol tunnel test section and the union nut was screwed down to a firm tightness.

operation, a Type G filter (Gelman, all-glass mat with supporting scrim, 47 mm diam) was placed in the holder, and its initial pressure drop was observed and recorded (approximately 2 in. of gage oil, sp.g. 0.826, at 0.97 cfm). Flow rate through the filter was measured by calibrated flowmeter "B" shown. A suspension of monodisperse solid particles in liquid was atomized by the sprayer system shown in Figs. 4 and 5.

Figure 4 is a schematic diagram of apparatus for the generation of the monodispersed solid aerosol particles. Four major components are illustrated: (1) a silica gel drying column, (2) a compressed air regulator valve, (3) a sprayer with a particle suspension reservoir, and (4) a drying section connected to a tee. Figure 5 contains details of the sprayer. Filtered compressed air

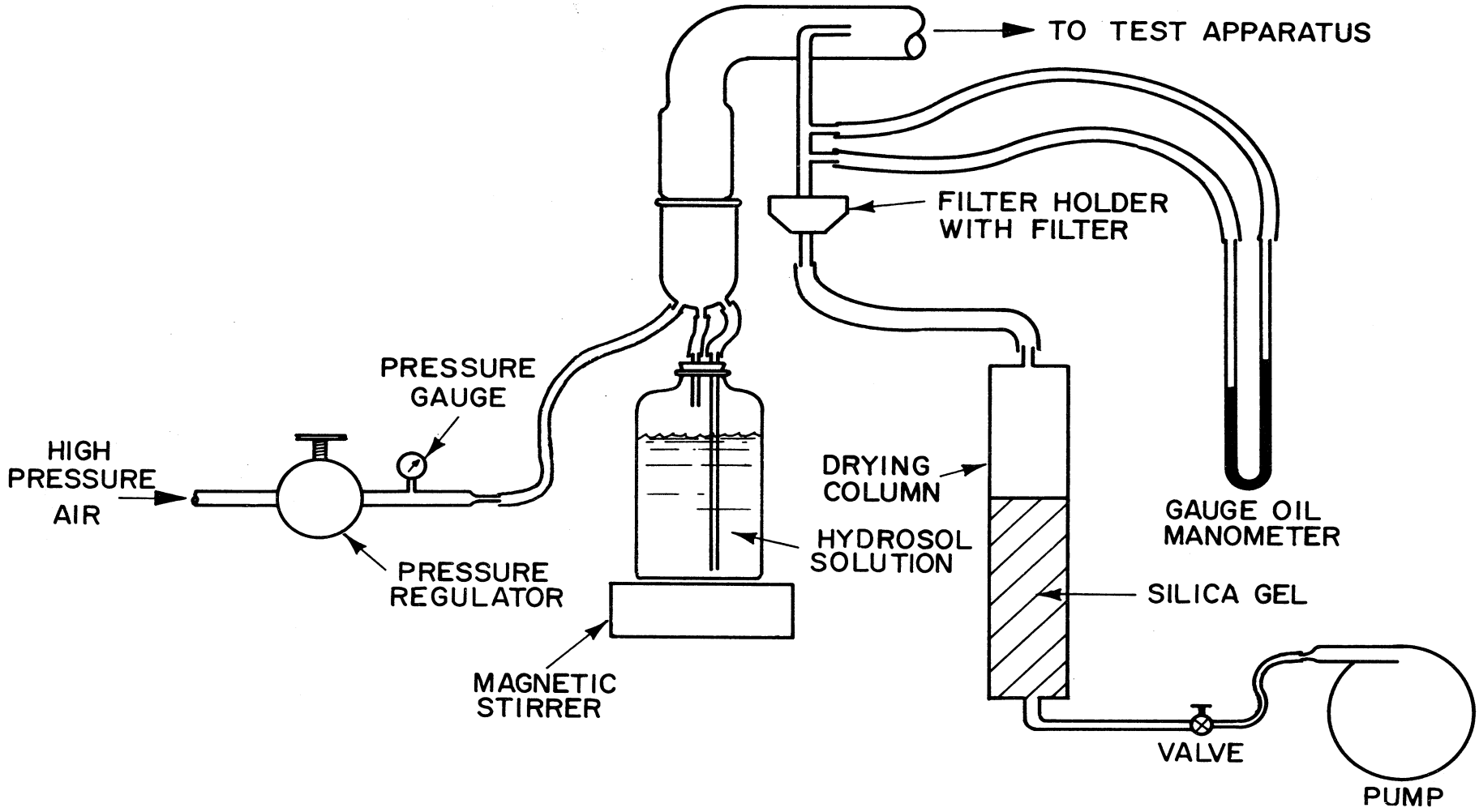

Fig. 4. Schematic diagram of aerosol generator.

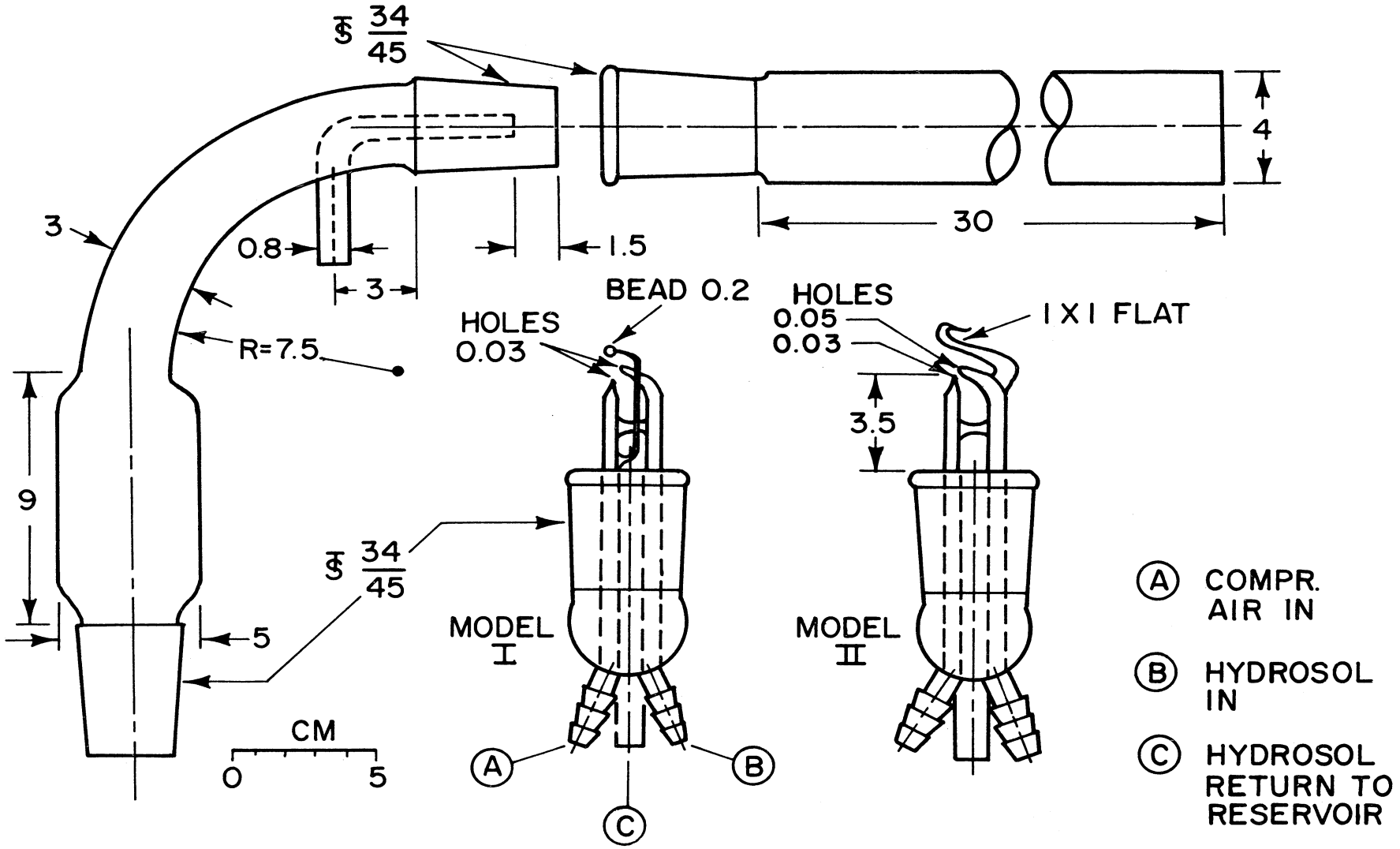

Fig. 5. Aerosol generator details.

was regulated and then passed through a hose to the sprayer. During the operation of model II generator, pressure was regulated to 60 psig; sprayer air volume was 13.7 lpm at laboratory temperature and pressure.

Liquid was supplied to the sprayer from the one-liter bottle located on a magnetic stirrer shown just below the generator, as shown in Fig. 4. Stock suspensions of Dow Polystyrene Latex Particles* were diluted with distilled, demineralized, and membrane filtered water. Dilutions ranged from 10^3:1 to 50:1 in the various tests.

The suspension was conducted from the reservoir bottle to the sprayer through a glass tube. The high velocity compressed air jet aspirated a stream of the hydrosol and atomized it by shear and by impaction on the adjacent surface. Most of the suspension deposited on the walls of the enlarged section of the elbow shown in Fig. 5. A fine mist passed upward through the elbow to the drying section. The sprayer had a liquid feed rate of about 50 cm^3/min at an air pressure of 60 psig. About 1 cm^3/min was aerosolized, the remainder passing back to the storage reservoir by gravity through a return tube. Ten cm^3/hr of dilution water was added to the reservoir to compensate in part for evaporation losses caused by the sprayer compressed air.

Dried air (33.3 lpm) was admitted through the smaller tube at the top of the elbow shown in Fig. 5. This air had been pumped through the silica gel column and then membrane filtered and metered. An aerosol of the monodispersed polystyrene latex spheres formed as the mist droplets evaporated in the straight tube section.

*1.305-μ diam, standard deviation 0.0158-μ, Run No. LS-464-E, Bioproducts Dept., The Dow Chemical Co., Midland, Michigan.

To measure the change in pressure drop caused by particle accumulation the flow was started at approximately 1 cfm through the filter and the aerosol generator and drying air were turned on. Excess aerosol was discharged through the tee connection shown in Fig. 1. Time and filter pressure drop were recorded periodically, and flow rate was maintained constant by means of the pinch clamp shown during test periods of a few minutes to a few hours.

Tests with liquid particles were performed in the same way as described above, but the silica gel dried air was not turned on. Spray from the generator was conducted directly to the test filter and pressure drop and time of operation were recorded.

When it was desired to check the particle concentration (i.e., number of particle per unit volume) of the flow, the tunnel-type filter holder was removed from the system and replaced by an open-type membrane filter holder with a .45 μ membrane filter. As before, the particle generator was turned on, and then the vacuum pump and stopwatch were simultaneously started. The test was run at steady flow conditions for a period of time (usually about 1 min), then the apparatus was turned off and the membrane filter removed. The filter was cut into quarters. One quarter was placed on a glass microscope slide. After adding a few drops of mineral oil the filter became transparent. The slide was then placed in a microscope with a 95x oil immersion lens and a 10x eyepiece. A 35μ x 35μ field was engraved in the eyepiece, and the number of particles within this size field could be easily counted. Six fields were counted, two near the center of the filter, two about halfway between center and edge, and two near the filter edge. The average number of particles per 35μ x 35μ field

was then computed. Since the diameter of the exposed filter surface was known to be 41 mm, it was possible to compute n, the total number of particles on the filter.

The total volume of air passing through the filter was Qt, and the particle concentration, N_o, was given by:

$$N_o = \frac{n}{Qt} \tag{10}$$

The value of N_o was found to be about 1600 particles/cc for the 50:1 dilution of the hydrosol.

2. Results of Solid Particle Accumulation Tests

The data for test 1 are shown in Table I. A graph of the results appears on Fig. 6. As predicted by the theory discussed above, the pressure drop rises linearly with time at first, then becomes nonlinear, and finally becomes asymptotic to another straight line.

The first linear period lasted approximately 1 hr. Concentration checks were made before, during, and after the run, and the slight jump in the curve at 130 min is due to disconnecting the tunnel-type filter holder for the concentration check. The results of these checks are:

Time (min)	N_o (particles/cc)	Variation from Mean (%)
0	1822	+7.3
130	1533	-9.7
252	1740	+2.5

The accumulation A of particles on the filter is given by:

TABLE I

RESULTS OF TEST 1

Time (min)	Filter Pressure Drop (in. g.o. (0.826)	Remarks
0		Initial Concentration Run: 2 min, N_o = 1822, flow kept constant thru test at 0.97 cfm
4	2.14	
10	2.23	
16	2.29	
21	2.34	
25	2.39	
30	2.45	
40	2.58	
41		Shut down
50	2.69	
60	2.82	Added 10 cc filtered water
93	3.34	
106	3.61	
124	4.01	Added 10 cc water, concentration test—removed fiber filter from holder, ran 2 min., N_o = 1533
130	4.16	
132	3.96	
136	4.08	
142	4.23	
156	4.62	
170	5.06	
180	5.43	Added 10 cc water
200	6.19	
220	6.99	
246	8.25	
252	8.52	Added 10 cc water, conc. run filter, end, 2 min, N_o = 1740

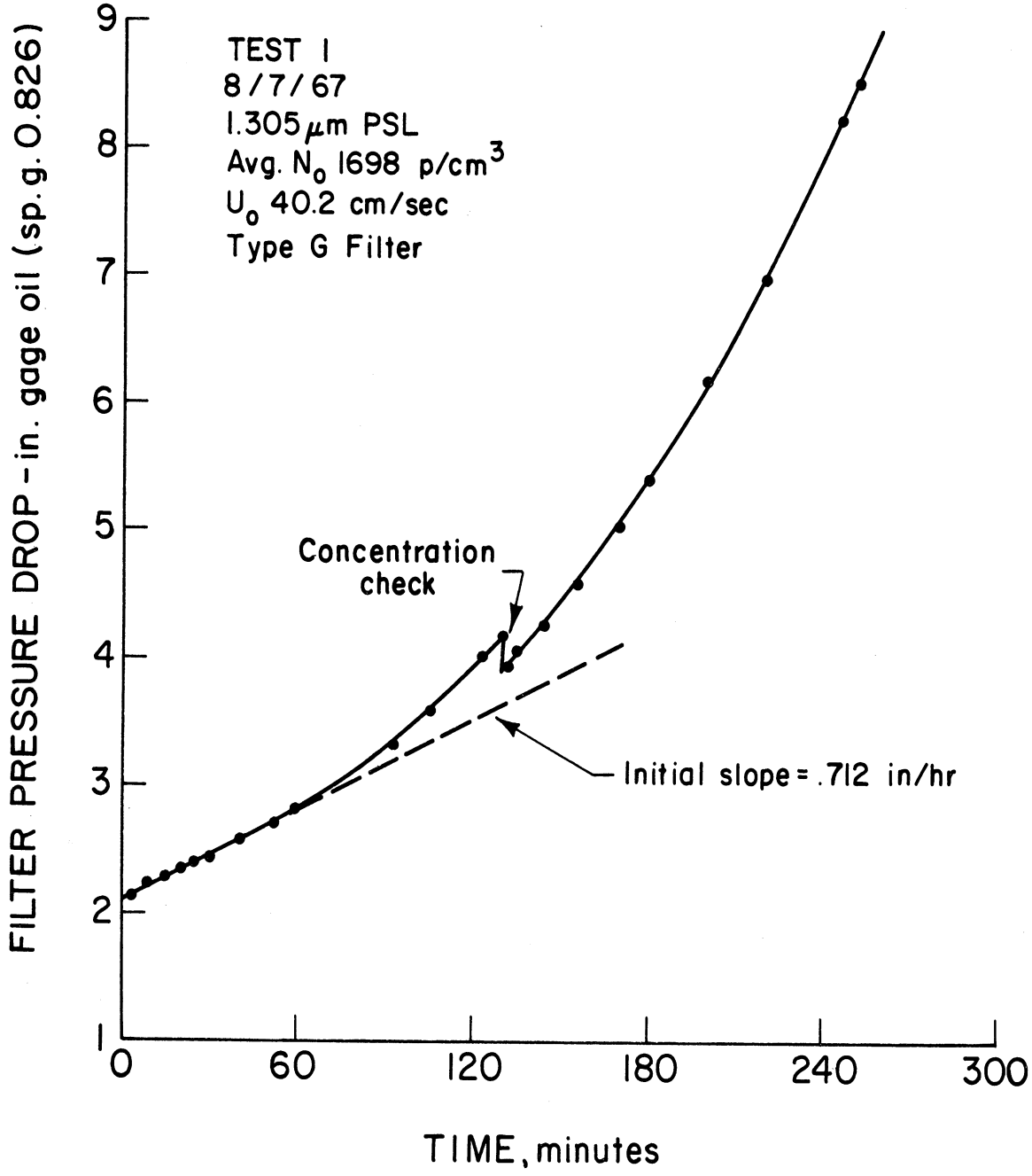

Fig. 6. Filter pressure drop as a function of time—test 1.

$$A = U_o N_o t \bar{E} \qquad (11)$$

where

U_o = flow velocity, cm/sec

N_o = particle concentration, p/cm^3

t = time, sec

$\bar{E}$ = efficiency of filter (fraction)

Flow velocity can be computed from

$$U_o = Q/K$$

where

Q = flow rate

K = filter area

With a flow rate of .97 ft^3/min and a filter diameter of 1.5 in., as in this test; U_o = 40.2 cm/sec. The mean of the three check runs was N_o = 1698 particles/cc.

A test to determine the efficiency of the glass fiber filter was run. A membrane filter was placed behind a fiber filter and a particle stream was allowed to flow through both filters. After 60 min of operation the number of particles on the membrane filter was very small, indicating that the particle concentration on the downstream side of the fiber filter was in the order of 4 particles/cc. Hence assuming $\bar{E}$ = 1.0 appears to be justified.

After 60 min of operation the accumulation on the fiber filter was A = 2.46×10^8 particles/cm^2 of filter face area.

Test 2 was run under the same conditions as test 1 with more data obtained during the first hour. Data for test 2 are given in Table II and a graph of these data is shown in Fig. 7. Particle concentration checks were made before and after the test, with the following results:

Time (min)	N_o (particles/cc)	Variation from Mean (%)
0	1550	-2.8
120	1640	+2.8

Note that the mean N_o in this test, 1595 particle/cc, is fairly close to the mean in test 1, 1698 particle/cc.

Again the pressure drop across the fiber filter rises linearly with time initially and becomes nonlinear after about 1 hr. The slope of the linear sectum, .69 in. of gauge oil/hr, compares with the slope found in test 1 of .71 in. of gauge oil/hr.

Using the same procedure to calculate the accumulation A as outlined in test 1, $A = 2.30 \times 10^8$ particles/cm^2.

Two preliminary tests were conducted at a lower velocity (~20 cm/sec) and a hydrosol dilution ratio of 10^3:1. Data from these tests is not reproduced here because of their tentative nature. Estimated particle concentration was 180 p/cm^3 (~2 million particles/cu ft, 1.305 μm). Filter pressure drop remained nearly constant over a 1 hr period. These low loading tests were discontinued and the aerosol was increased (to 45 mppcf, 1.305 μm) with results as reported above. The calculated slope for the increase in pressure drop for the low loading test was (0.70/22.5x2 in. gauge oil/hr) 0.015 in./hr. The base (ini-

TABLE II

RESULTS OF TEST 2

Time (min)	Filter Pressure Drop (in. g.o. (0.826)	Remarks
0	2.14	Initial Conc. check N_o = 1550 p/cm^3
2	2.16	Flow kept constant through test at 0.97 cfm
4	2.20	
6	2.21	
8	2.25	
10	2.27	
12	2.29	
14	2.31	
16	2.35	
18	2.36	
20	2.38	
22	2.40	
24	2.42	
26	2.44	
28	2.47	
30	2.49	
35	2.55	
40	2.60	
45	2.67	
50	2.73	
55	2.79	
60	2.85	
65	2.93	
70	3.02	
75	3.11	
80	3.17	
85	3.26	
90	3.37	
95	3.47	
100	3.59	
107.5	3.78	
110	3.85	
115	3.99	
120	4.15	Final conc. check, N_o = 1640 p/cm^3

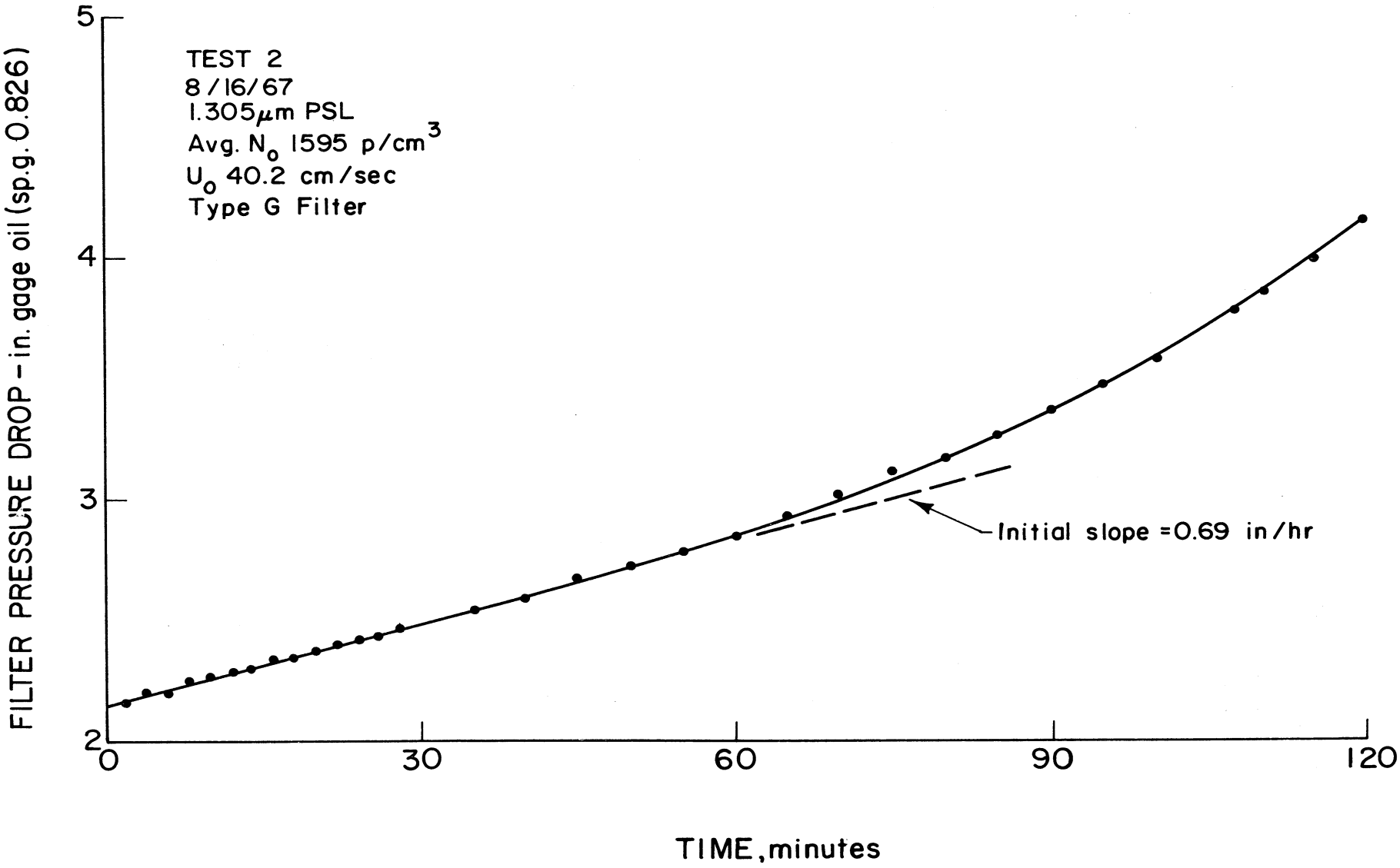

Fig. 7. Filter pressure drop as a function of time—test 2.

tial) pressure drop of the clean filter was about 1.0 in. of oil, and the slight increase in pressure drop of 0.01 in. gauge oil was difficult to quantitate in a 1 hr test.

3. Discussion of Results

Results indicate that the theory presented above (Section A) is quantitatively correct. The initial slope of the filter pressure drop-time curves for two separate filters was found to be essentially linear, at 0.712 in. gauge oil/hr (1698 p/cm^3) and 0.690 in./hr (1595 p/cm^3), respectively. The particle resistance coefficients, S_p, calculated from these data and Eq. (8) are 12.62 and 13.01, respectively. These results are similar to those calculated from data of LaMer (discussed in (1), p. 70). His data for wax particles of diameter 0.365 μm at 10^6 p/cm^3, $4.7 \leq U_o \leq 28$ cm/sec, yields an average value of 13.6 for S_p. The fiber fraction (α) in his test filters was estimated to be 0.128. The fiber fraction was calculated for the Type G filters used in the present study (exclusive of scrim) and found to be approximately 0.093. Values of the particle coefficient found in this study and in the study by LaMer do not agree with the empirical relationship given for less dense filters in Eq. (9), $S_p = 33\alpha$ $(0.007 < \alpha < 0.035)$. Evidently this relation is not linear and must be modified for higher packing densities. In any case, it is apparent that a more compact filter (higher α) produces a higher resistance per unit of accumulated material. The storage capacity of a denser filter is lower than for a more loosely-packed filter as reflected by its higher resistance rise per unit of accumulated particle material.

The resistance rise of the filters tested in this study was intially linear, as predicted by the assumption that the particles are "far" apart and not interacting strongly with the flow field within the fibrous filter. After test operation of an hour or so, the resistance increase became nonlinear for a period of 2 to 3 hr (in one test). Beyond this point, the resistance appeared to approach linearity again. This behavior would be anticipated, as particles deposit and begin to close up the interstitial spaces between the filter fibers. A porous medium of deposited material should form on the front face of the filter. At this time the deposit growth will be similar to that found in fabric industrial dust and fume collectors, where the deposit is the primary structure for filtration (e.g., a filter "cake" forms). The analysis of this part of the filtration process has been given by Williams, Hatch, and Greenberg in the form[2]:

$$\delta\Delta p = HU_o^2 ct \qquad (12)$$

where

H = "specific" dust resistance coefficient, inches water/lb of dust/sq ft of fabric/min/ft/min filtering velocity,

c = dust concentration, lb/cub ft.

Values of H for various fabrics and various industrial dusts have been reported in the range of 40 to 80. The form of the empirical function (Eq. (12)) agrees with the theoretical prediction for the initial stages of the process when the particles are far apart. Apparently the fiber fraction influences the coefficient in the early stages of the filtration process in a fibrous filter, and the intrinsic (Darcy) permeability of the deposited dust layer affects the value of the "specific" dust resistance coefficient in the later stages. Similarities

between the theoretical and empirical resistance equations have not been investigated as part of this study. The value of H for data of Test 1 is 42, during the period 220 to 260 min, for a calculated dust loading of 8.6×10^{-4} grains/cu ft. The coefficient is within the range found for industrial dusts.

In summary, results of the particulate accumulation tests are consistent with other studies, and the linear behavior predicted by theory has been confirmed. This approach appears to be feasible for the design of a continuous automatic aerosol monitor.

4. Effects of Liquid Spray Droplets

During the tests described above with solid particles, an experiment was conducted with liquid spray droplets from the sprayer by leaving the drying air supply off. It was found that resistance rose very rapidly during a few minutes. The plot of these data were linear. Because the drying air had been omitted due to an experimental error, these data were discarded. Upon further reflection, it appeared possible to adapt the proposed aerosol monitor development for the measurement of liquid aerosol particle concentrations, in applications such as tar droplets or spray dust collector effluents. Two additional tests were run with spray droplets to evaluate the effect on filter pressure drop.

In test 3 the dry air stream after the particle generator was not turned on. The filter was exposed to a stream of water droplet, rather than a stream of solid particles in air. The rise in pressure drop was quite fast. Two runs were made in this test under what was hoped were the same conditions. However,

the results were different, as can be seen from the graph on Fig. 8. Data for this test may be found in Table III.

It was not possible to reproduce the linear relation between pressure drop increase and operating time. The method may have some application for liquid droplets, but it is not possible at this point to confirm the linear behavior. Further study is required to quantitate the spray droplet concentration (unknown, approximately 1 gm/min) and size distribution (estimated in the range 1 to 5 μm, based on the high pressure used in the generator). It may also be possible to determine mixed aerosols with solid particle content and liquid particle content on the same filter by programming the sequence of pressure drop measurements with an intermediate drying operation.

TABLE III

RESULTS OF TEST 3—SPRAY DROPLETS

Run A		Run B	
Time (min)	Filter Pressure Drop (in. g.o. (0.826))	Time (min)	Filter Pressure Drop (in. g.o. (0.826))
15 sec	2.74	0	2.40
30	3.01	30 sec	2.67
60	3.72	45	2.88
1:15	4.15	1:00	3.09
1:30	4.62	1:15	3.39
1:45	5.20	1:30	3.66
2:00	5.99	1:45	4.03
2:15	6.65	2:00	4.39
2:30	7.70	2:15	5.01
2:45	9.85	2:30	5.38
		2:45	5.89
		3:00	6.57
		3:15	7.32
		3:30	8.55

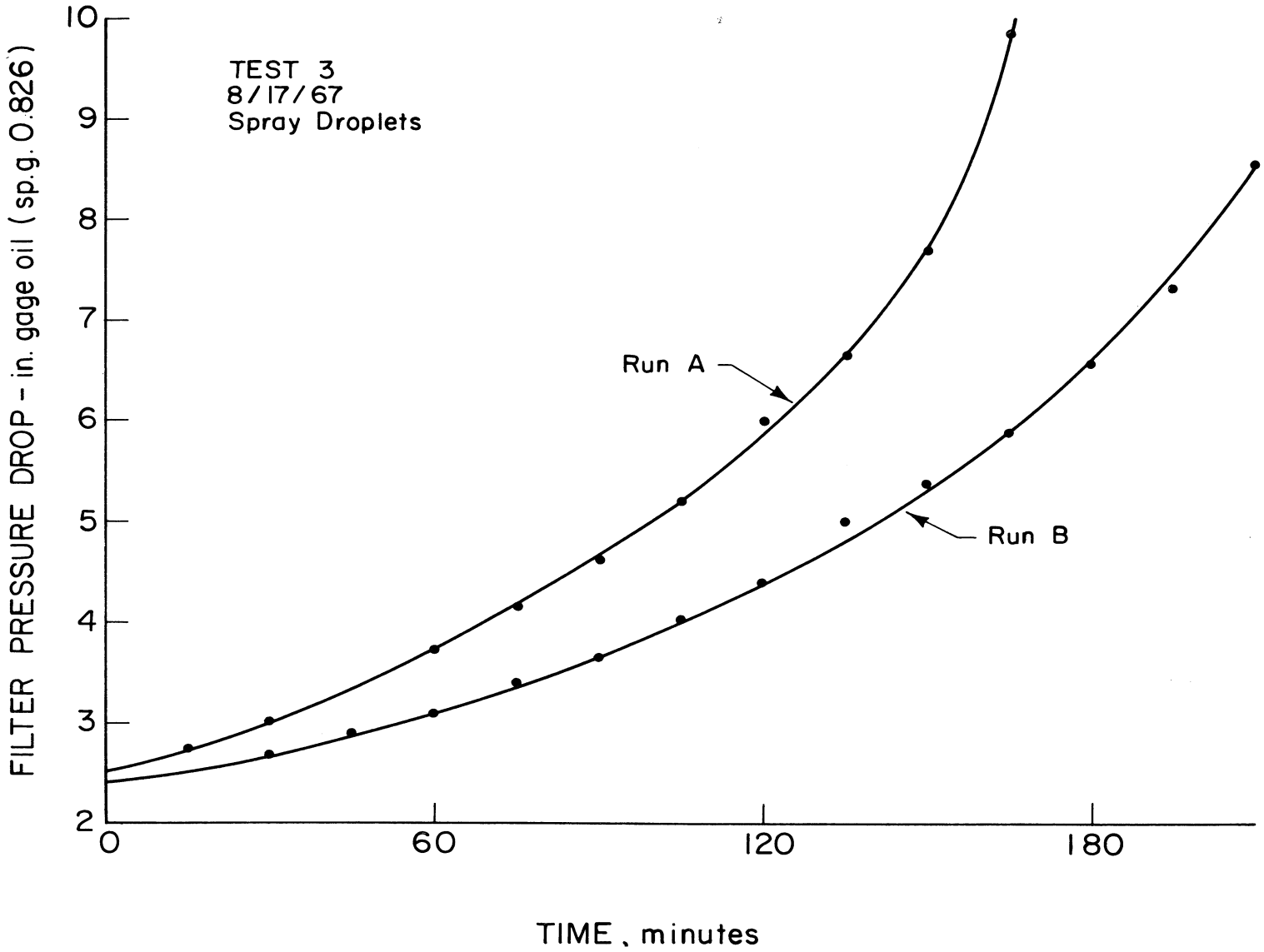

Fig. 8. Filter pressure drop as a function of time—spray droplets—test 3.

III. SIGNAL TREATMENT AND DATA REDUCTION

A. PRESSURE SENSING SYSTEMS

1. Transducers

The essential physical process used in this development is described above. A filter mat is placed in the path of a stream of air and causes a static pressure drop $\Delta p(0)$. An additional pressure drop $\delta\Delta p(t)$ arises as particles in the air stream deposit on the mat. The total pressure drop across the filter is then:

$$\Delta p(t) = \Delta p(0) + \delta\Delta p(t) \qquad (13)$$

The increment in pressure drop, $\delta\Delta p(t)$ is related to the amount of deposited material, and must be separated from the total pressure drop. Several systems have been considered for this purpose. The simplest procedure would be to record $\Delta p(0)$ at the start of filtration and subtract it from $\Delta p(t)$ after a fixed interval of filtration, t. This method of data treatment would be essentially the same as used for the evaluation of tape stain data. (Reduction in light transmission caused by a stain is currently used as an arbitrary index of atmospheric pollution, but is not simply related to particle concentration in the air.) The utility of the proposed monitor derives from automatic quantitation of the output in terms of mass or number concentration.

Two other methods of data treatment have been considered: direct differentiation of the signal from a pressure transducer; and subtraction of two

electrical signals from a pressure transducer at differing times. Both of these methods rely upon the linear relationship between $\delta\Delta p(t)$ and t shown above, and each gives the slope of the line, which is a unique function of particle concentration. Differentiation presently appears to present difficulties since the output noise increases in the differentiated signal. The sample ($\Delta p(0)$), hold (during t), and subtract method is discussed below.

To determine the increment $\delta\Delta p(t)$, the static pressure from each side of the filter paper will be connected to a pressure transducer.[3] The difference in pressure will cause a variation of a parameter in an electrical bridge circuit. This produces an electrical signal proportional to the static pressure difference (Δp). Various mathematical transformations can be performed on the electrical signal by using the properties of operational amplifiers[4]; including inversion, integration, differentiation, multiplication, division, and sample, hold, and compare difference.

The transducer consists of an enclosed membrane separating two pressure regions, an electrical bridge, a source of AC power, an amplifier, and a demodulator (AC-DC converter) to drive an output device (a recorder, or other signal treatment systems). Several kinds of transducers of varying sensitivities and principles of operation have been considered for this application as shown in Table IV. The operation of a typical capacitance transducer is shown in Fig. 9. The capacitance C is given in terms of the physical properties of the device as:

$$C = \frac{\epsilon A}{d} \tag{14}$$

where ϵ is the permitivity of the insulation between the plates, A is the plate

TABLE IV

PRESSURE TRANSDUCERS

Name	Manufacturer	Model	Range	Sensitivity*	Type	Approx. Cost
Bi-Directional Differential Gas Pressure Transducer	Hewlett-Packard	270	± 400 mm H_2O		Variable Reluctance	$1,000.00
Differential Pressure Transducer	Pace Wiancko	P7	± 0.1 - ± 500 psi		Variable Reluctance	535.00
Precision Pressure Gauge	Texas Instrument	144-01	0 - 5 psi	0.001% F.S.	Quartz Tube	2,085.00
Baratron	MKS Instruments	77H-300	± 300 mm Hg	0.001% F.S.	Variable Capacitance	2,475.00
	Lion Research	DC-303			Variable Capacitance	650.00
Quartz Pressure Transducer	Kistler	701A	0.01 to 30 psi	0.01 psi	Piezo-Electric	1,200.00
Semi Conductor Pressure Transducer	Consolidated Electrodynamics	4-420			Semi-Conductor	
Pressure Sensor	Rosemount Engineering	1101				
Digital Pressure Gauge	Robinson-Halpern	620 A/B				
	Viatran	PT B304				
	Metrophysics	10311	0.001 to 30 mm Hg			
	Scientific Advances	SA-SA M-65	± 2 psi			

*F.S.—full scale

Note: Prices shown include auxiliary equipment—amplifiers, demodulators, etc.

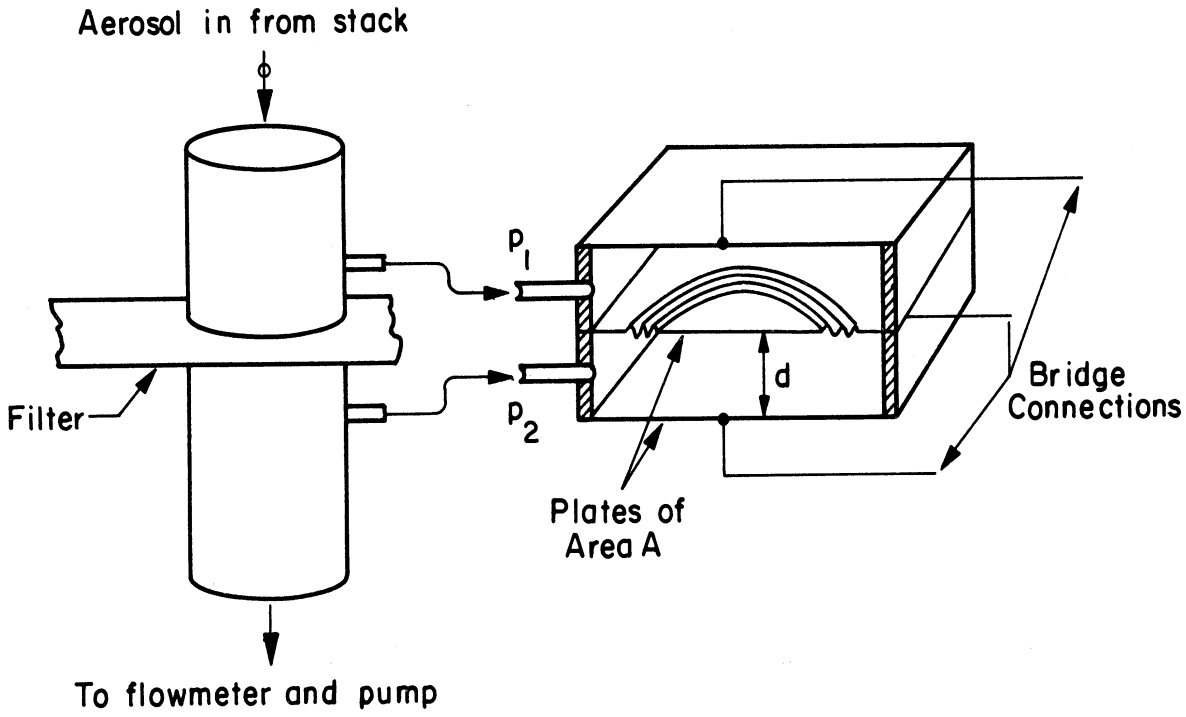

Fig. 9. Schematic of capacitive transducer.

area, and d is the plate spacing. A change in pressure causes a displacement Δd. The corresponding change in capacitance causes an unbalance in an electrical bridge circuit. The bridge is energized with an AC voltage, as shown in Fig. 10. The output signal is amplified and demodulated in the carrier amplifier.

Operation of the other types of transducers listed in Table IV depend upon other physical systems such as the Bourdon tube, piezoelectric effect, or the properties of semiconductors. An inductive or capacitive transducer seems satisfactory for the purposes of this development. The desired pressure signal will be of order 0.1 in. of water on a background differential pressure of order 1 to 10 in. of water, which is well within the range of sensitivity of

these devices. Transformation of the electrical signal output from the carrier amplifier is discussed below.

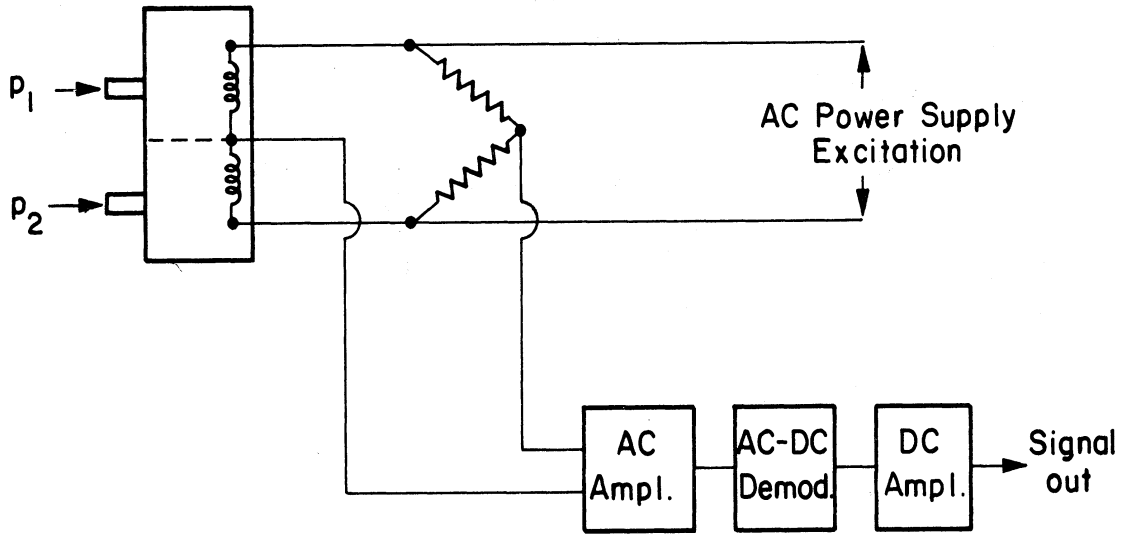

Fig. 10. Schematic of transducer electrical circuit.

2. Pneumatic Bridge

Another approach to detecting the accumulation pressure drop $\delta\Delta p(t)$ is to use it to produce a flow system change and measure the flow. A device using this principle for detection of water vapor has been described by Wildhack, et al.[5] Their critical-flow bridge development is shown in Fig. 11. It appears to have application for detection of particulate and gas concentrations. Four critical flow orifices are arranged in two parallel branches, each branch containing two orifices. A device which collects the desired component of the aerosol stream (e.g., a filter for particulates, an adsorbent for gases, or a dessicator, as shown) is placed between the upstream and downstream orifices in one branch. Mass flow rate through the downstream orifice is proportional

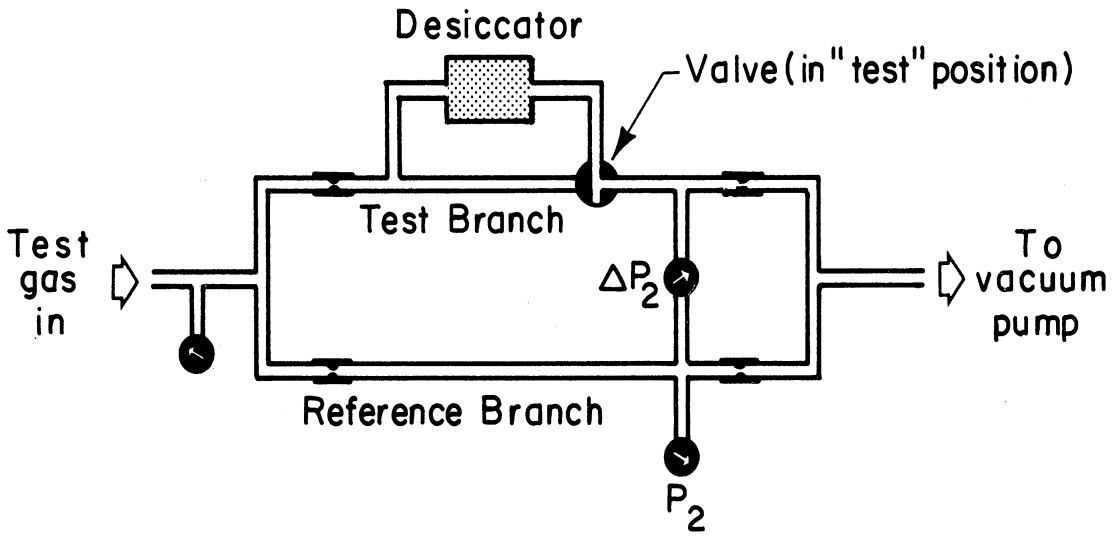

Fig. 11. Critical-flow bridge.

to the upstream pressure only, so that the change in mass flow caused by the adsorption of a gaseous component (e.g., moisture, SO_2, NO_2, etc.) or the change in pressure caused by the deposit of particles in a filter placed in the stream, will affect the intermediate pressure in the test branch. The intermediate pressure in the test branch is then compared with that in the other (reference) branch by means of a differential manometer or transducer, ΔP_2. From this measurement, together with the absolute pressure P_2, the change in concentration produced by the device in the test branch may be calculated. The design of critical-flow orifices for this application are discussed in the Wildhack article.[5]

A pneumatic analog Wheatstone Bridge circuit is shown in Fig. 12. Aerosol flow enters the bridge and splits into two streams, passing through equal sharp-edged orifice resistances, $\Delta p_1 = \Delta p_2$. Filter paper is mounted in the third arm and gives rise to a pressure drop Δp_3 at the start of filtration. Pressure

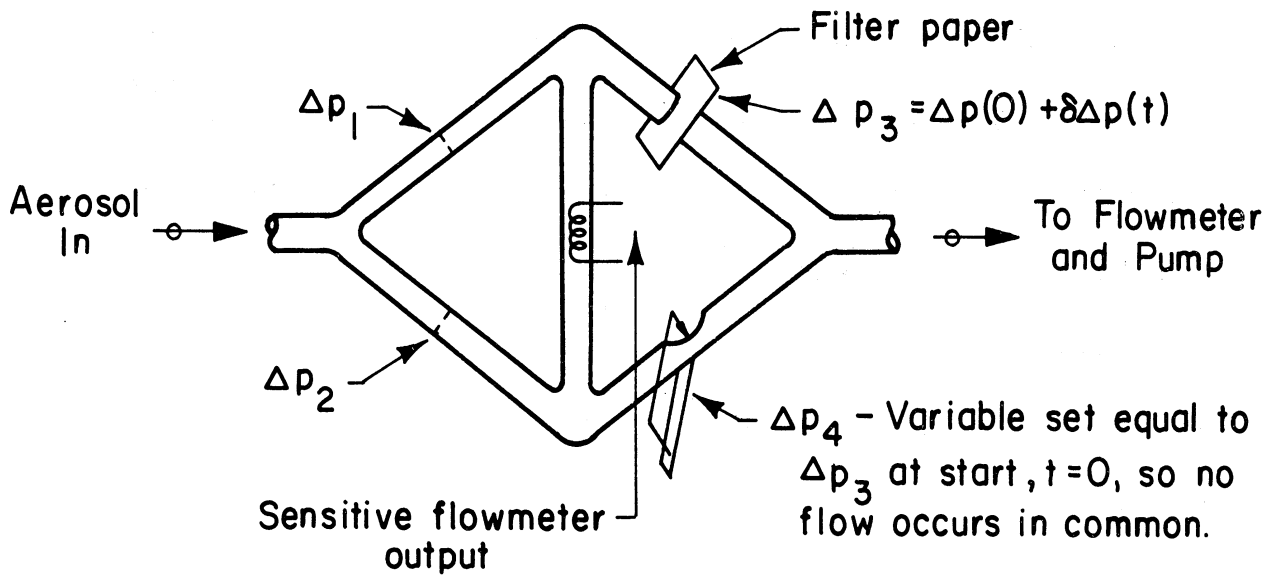

Fig. 12. Analog pneumatic bridge.

drop in the fourth arm of the bridge, Δp_4, is made equal to Δp_3 by a variable flow resistance controlled by a sensitive thermal or ion flowmeter in the common connector. The bridge is balanced at the start of operation ($\Delta p_3 = \Delta p_4$), so no flow occurs in the common connecting line, and the null condition is the signal used to vary resistance Δp_4. As particles accumulate as the filter paper, Δp_3 will increase and produce flow in the common connector. This flow is related to the increment in pressure drop $\delta\Delta p$ caused by the accumulated deposit. The electrical signal from the flowmeter can then be used as input to the data handling system. Bridge operation depends upon a pneumatic zero suppression servo-loop (to set $\Delta p_3 = \Delta p_4$ at $t = 0$) in a configuration similar to that to be discussed below under electronic designs. These devices are currently under consideration for application to this development.

B. PROPOSED SYSTEM

The following discussion is concerned with methods for treatment of the electrical signal from the pressure transducer carrier amplifier. The proposed system will consist of operations shown in Fig. 13. The basic problem from the signal manipulation viewpoint is the separation of the component of the pressure signal proportional to $\delta\Delta p(t)$. The expected form of the signal $\Delta p(t)$ is shown in Figs. 6 and 7, assuming the transducer output signal is a linear function of the differential pressure input signal, for small differentials.

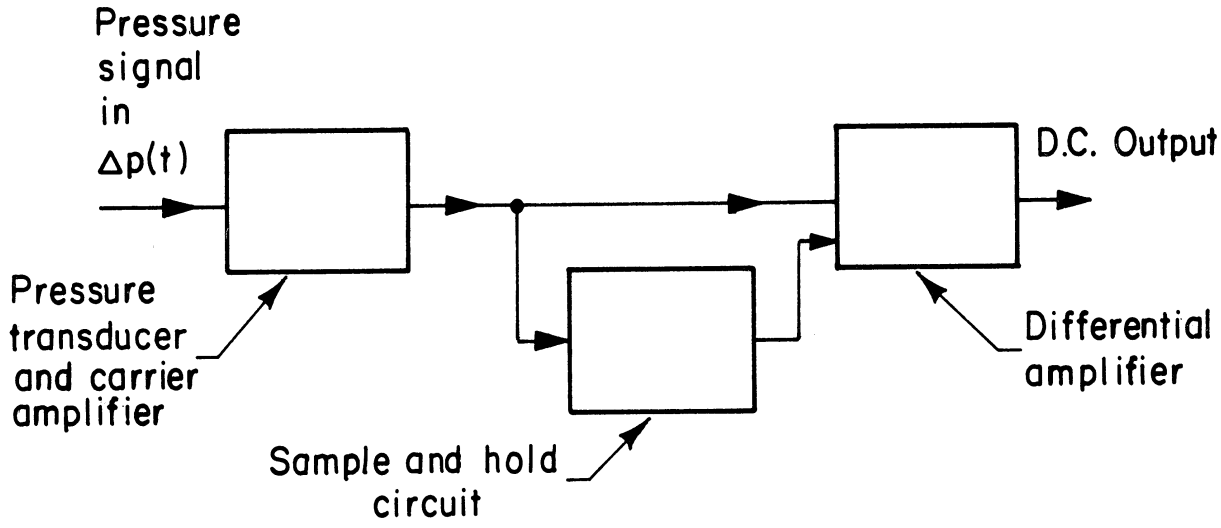

Fig. 13. Proposed signal treatment schematic.

At the start of a sequence of operations, the output of the pressure transducer is sampled and stored for the duration of the measurement in the sample and hold circuit as an electrical signal proportional to the initial filter pressure drop. While particles are depositing on the filter to cause the incremental pressure $\delta\Delta p$, the output signal from the transducer can be continuously compared to the initial sampled value, and their difference amplified by the differential amplifier. This output can then be recorded. The shape of

the output would be similar to records obtained from continuous in situ measurements of optical density on tape stain samplers equipped with an integral light source and photocell (e.g., Research Applicance Co., Model F-2-Ser A151 Sampler with builtin evaluator and recorder). Since the signals involved change slowly it will be possible to simulate the above operation manually by taking advantage of special features of the carrier amplifiers to perform the equivalent of the sample, hold and subtraction operations. A manual zero suppression feature is incorporated in the Hewlett-Packard carrier smplifier, and could be made automatic by a servo-loop system sampling $\Delta p(0)$.

Several configurations have been considered for the sample and hold circuit. The design suggested by Bulba and Silverman[6] is shown in Fig. 14. In this application of the operational amplifier, the capacitor C is charged with a voltage proportional to the initial filter pressure drop, $\Delta p(0)$, while the switch is closed ("sample" operation), the switch is opened (by a program timer) during pressure rise of the filter paper, and then the switch is closed again to compare the signals from the pressure transducer at a later time. The output would then be a single voltage proportional to the amount of accumulated material, and can be recorded (analog or digital) to represent the concentration directly by multiplication with the appropriate scale factor.

Consider the model sample and hold circuit shown in Fig. 15(a). Closure of switch B for a short time interval charges the capacitor C to the voltage e_{SO}. When the switch is opened the capacitor discharges into the amplifier exponentially. In Fig. 15(b) the resistor R represents the input impedance of the amplifier. By Kirchoff's current law we have:

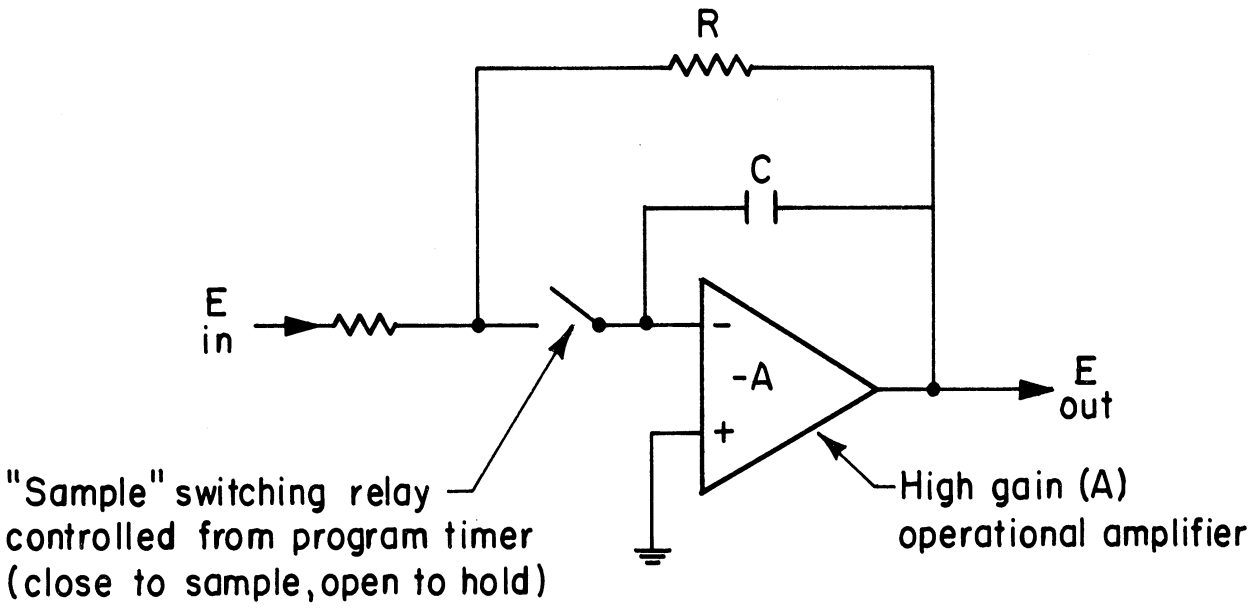

Fig. 14. Sample and hold circuit.

$$C \frac{de_{in}}{dt} = - \frac{e_{in}}{R} \tag{15}$$

and

$$e_{in}(t) = e_{s_o} \exp(-t/RC) \tag{16}$$

Expanding the exponential in a Taylor series gives $e_{in} \cong e_{s_o}(1-t/RC)$. Thus initially e_{in} starts at e_{s_o} and decays linearly. For time intervals much smaller than RC we will have $e_{in} \cong e_{s_o}$, that is, the circuit will hold the sampled value. Thus if we desire e_{in} to remain within a factor ρ, $0 < \rho < 1$, of e_{s_o} for a time interval $0 < t < t$, then:

$$t_1/RC = 1 - \rho \tag{17}$$

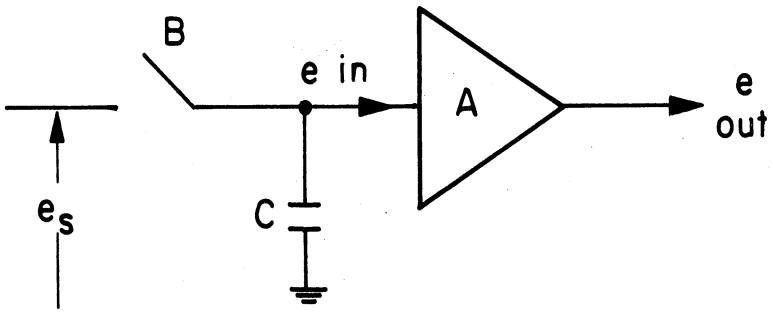

(a) Sample and Hold Circuit Diagram

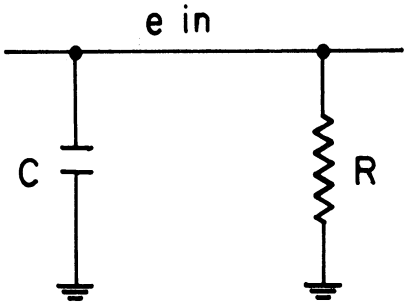

(b) Equivalent Input Circuit

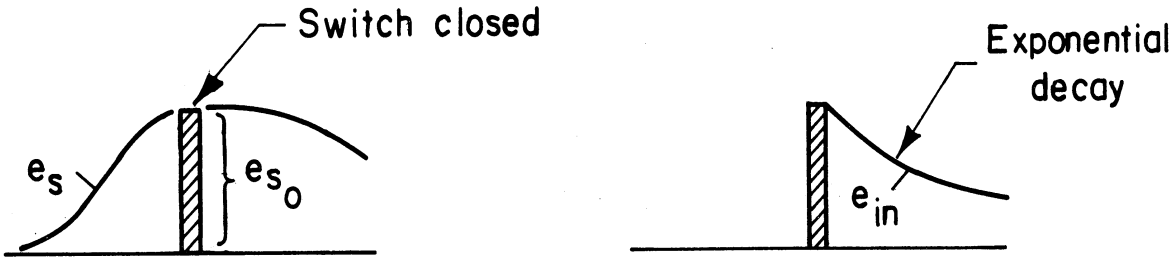

(c) Variation of Signal Voltage

Fig. 15. Sample and hold circuit operation.

or $t_1 = (1-\rho)RC$ is the allowed hold time.

For example, if R = 10k, C = 1 μf and we desire e_{in} to be .95 of e_o, or better, then we obtain for the hold time $t_1 = (1-\rho)RC = (0.05)(10 \text{ milliseconds})$ = 0.5 millisecond.

Note that the hold time interval increases with the RC product. That is, in order that the approximation $e_{in}(t) = e_{s_o}$ be valid for as long a time as possible it is desirable to have RC correspondingly large. However, there are practical limits to the value of the RC product. Increase in the value of R usually means increased cost and complexity of the amplifier, while increased C cause a heavier load on the $e_s(t)$ source during the sampling time. The use of an operational amplifier circumvents these limitations to some extent.

Basically an operational amplifier is an amplifier with a high open-loop gain. In ordinary use, feedback elements, resistor, inductor, capacitor are combined with the amplifier to produce devices which perform some mathematical operation on the input signal. The simplest configuration for its use in a sample hold circuit is shown in Fig. 15(a). Here no attempt has been made to show the necessary sampling circuitry. Assume that the sampled signal is initially allowed to charge the capacitor C. The analysis of the "hold" performance proceeds as follows:

$$e_o = -Ae_i \tag{18}$$

$$C\frac{d(e_o-e_i)}{dt} = \frac{e_i}{R} = -\frac{e_o}{AR} \tag{19}$$

or

$$C\left(1+\frac{1}{A}\right)\frac{de_o}{dt} + \frac{e_o}{AR} = 0 \tag{20}$$

At the termination of the sampling time we have $e_o - e_i = E_o$. Combining this with Eq. (18) gives $(\frac{1}{A} + 1)e_o = E_o$ or $e_o = E_o(1/1 + \frac{1}{A}) \simeq E_o$ for A (amplifier gain) very large. Thus from Eq. (20):

$$e_o(t) \simeq E_o e^{-t/ARC(1 + \frac{1}{A})}$$
$$\simeq E_o e^{-t/ARC} \qquad (21)$$

It is seen that the simple RC time constant is multiplied by the open-loop gain of the operational amplifier, thus improving the hold operation time. A typical calculation will indicate the improvement obtainable. If R = 15,000, C = 1 μf and A = 15,000, then $1/\lambda = ARC = 10^{-6} \times 15{,}000 \times 15{,}000 = 225.0$ sec. For $0 < t < 2.25$ sec, $e(t) = E_o$ within 1%. With the same RC values in the simple sample hold circuit considered previously we have $1/\lambda = (15{,}000)(10^{-6}) = 15$ msec. For a 1% decay the time interval is then about 0.15 msec. The operational amplifier thus has the effect of increasing this time by the open-loop gain. Amplifiers with gains of 10^6 or greater are available, so the holding time can be increased to 10^3 sec.

The operational amplifier which is proposed to use is of the differential type in which the output is proportional to the difference of the two input signals. A similar analysis to that given above shows that a similar relationship is obtained for the effective time constant of the configuration. Figure 16 shows these configurations and effective time constants.

C. EXPERIMENTS

Since the pressure transducers and associated equipment had not been selected at the outset of this research, it was decided to simulate the operation

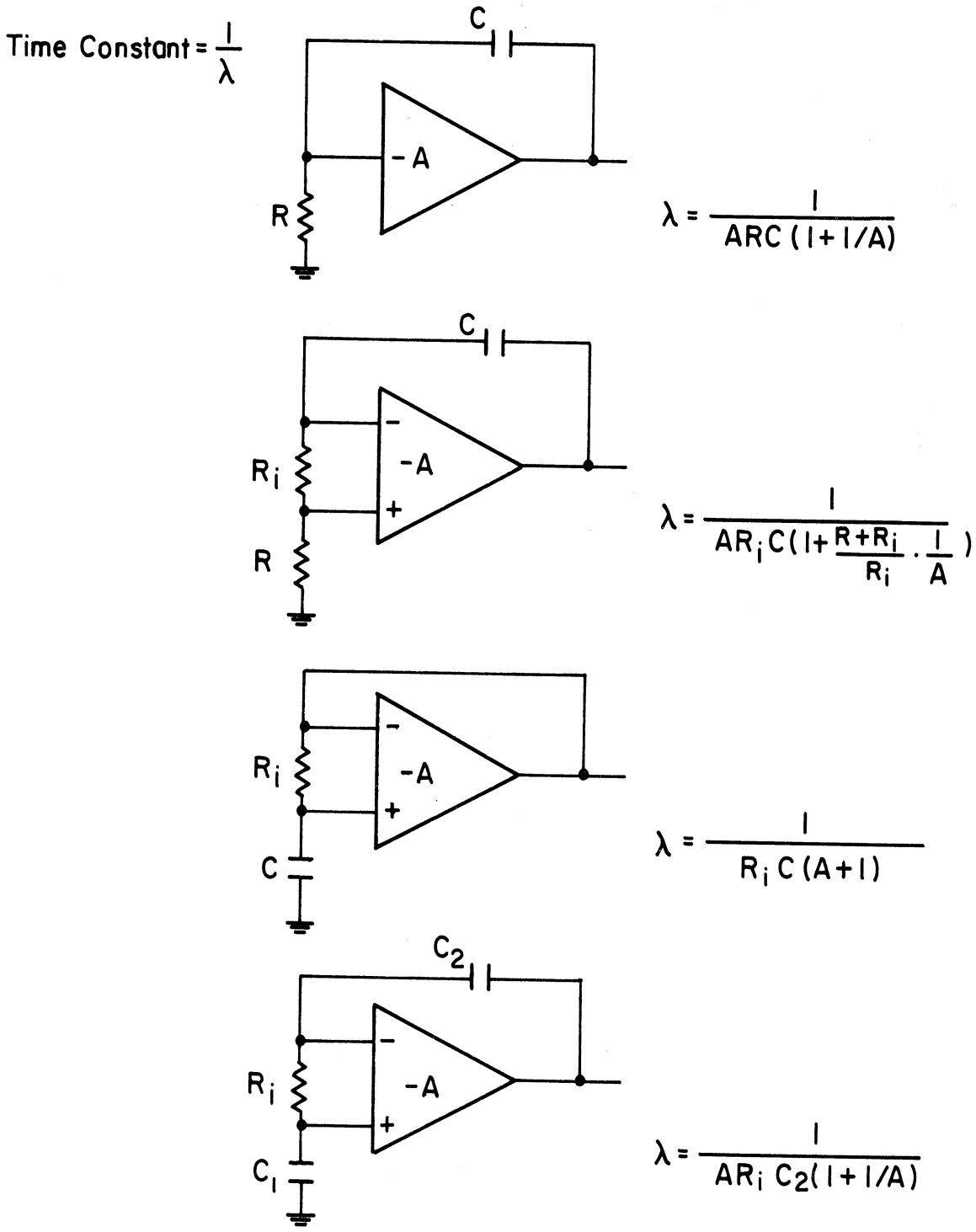

Fig. 16. Time constants for sample and hold circuits.

of the transducer electronically in order to study performance of different operational amplifiers. The simulation circuits are shown in Fig. 17. The purpose of the circuit shown in Fig. 17(a) is to simulate the signal $\Delta p(t)$, that is, a signal increasing linearly with time. Switch 1 is closed momentarily and capacitor C_A charges to the voltage E. When the switch opens the output voltage will start at E and decay with a very long time constant. For a short time interval the decay will be linear, simulating a $\Delta p(t)$ with a linear decrease (i.e., the inverse of the actual pressure signal). This circuit was built using an RCA CA3030 integrated operational amplifier, but without much success. With C = 0.1 μf a decay time constant of 1.5 sec was expected. The actual circuit performance consisted of a linear decay which took about 150 msec. A multivibrator circuit was designed and constructed to supply periodic impulses to relays controlling the simulated sample and hold circuit.

The circuit design shown in Fig. 17(b) was not tested. Difficulties with the first simulation circuit (17(a)) appeared to be due to low input impedance on the RCA CA3030 amplifier, its comparatively low gain, and improper specification of its input bias. Improved operational amplifier performance can be anticipated from the Philbrick configurations, at substantially higher cost (about 20 times greater). Characteristics of these better amplifiers seem to be more suitable for this application requiring a hold time of several minutes. In addition, we are currently investigating commercial sources of complete sample-hold modules.

All of the above circuits are simpler than those proposed by Bulba and Silverman.[6] The signal treatment used in this present study does not require

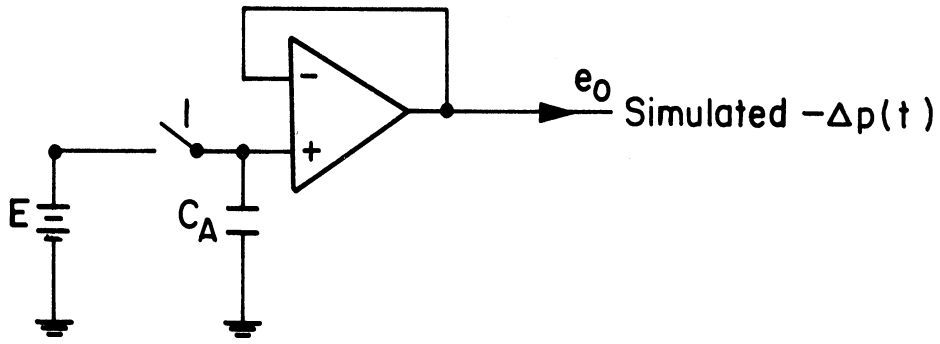

(a)

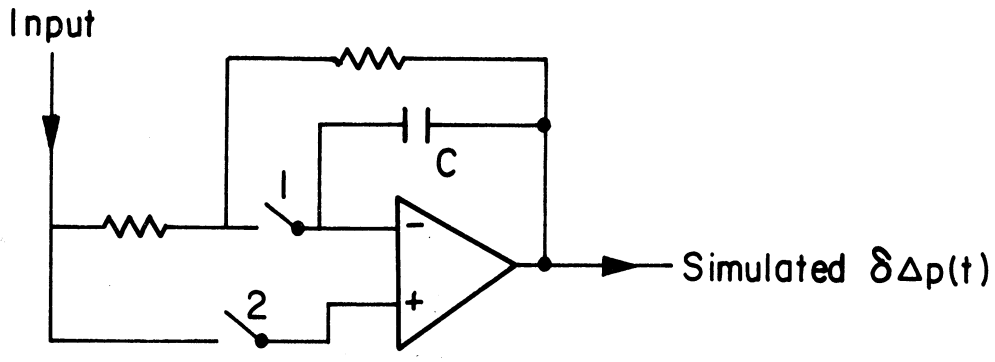

(b)

Fig. 17. Simulation circuits.

a rate meter analog step nor a logarithmic feedback loop. The signal from the pressure transducer is a linear function of time and concentration. The β-guaging technique used by Bulba and Silverman depends upon logarithmic penetration of the radiation through the deposit to the detector tube. In addition to being simpler, the method proposed here does not require that a sealed source of radiation be acquired and accounted for in every instrument. This reduces a personnel hazard or accident situation.

IV. FUTURE STUDIES

A. FLOW NOZZLE DILUTER

For certain applications, it may be desirable to dilute the particulate sample to reduce the particle concentration before it reaches the filter. Dilution can also reduce condensation of moisture in the sampling lines from the stack and at the filter. It also may be utilized to eliminate particulate deposition on the wall of the sampling probe prior to filtration at the continuous aerosol monitor. A flow nozzle diluter has been conceived for this purpose as shown in Fig. 18. It consists of two concentric tubes having a continuous flow of compressed air or gas in the annulus between them, as shown. The stack sample containing condensable vapors or particulates to be diluted is admitted through the flow nozzle and combined with the dilution stream in the aerodynamic smooth entry sampling line. A boundary layer will form on the wall of the inner tube from the clean dilution gas and constrain the sampled stream to flow in the center of the sampling line until turbulence develops. The annular counterflow configuration for admission of the dilution gas will also provide some heat transfer possibilities. Diluted aerosol is conducted out of the diluter to the aerosol monitor filter system located adjacent to the stack. The pressure transducer can be located in a remote location at ambient temperature, if necessary, since pressures can be transmitted through tubing. The diluter configuration will be given further development. It is based on a suggestion by Washimi and Asakura.[7]

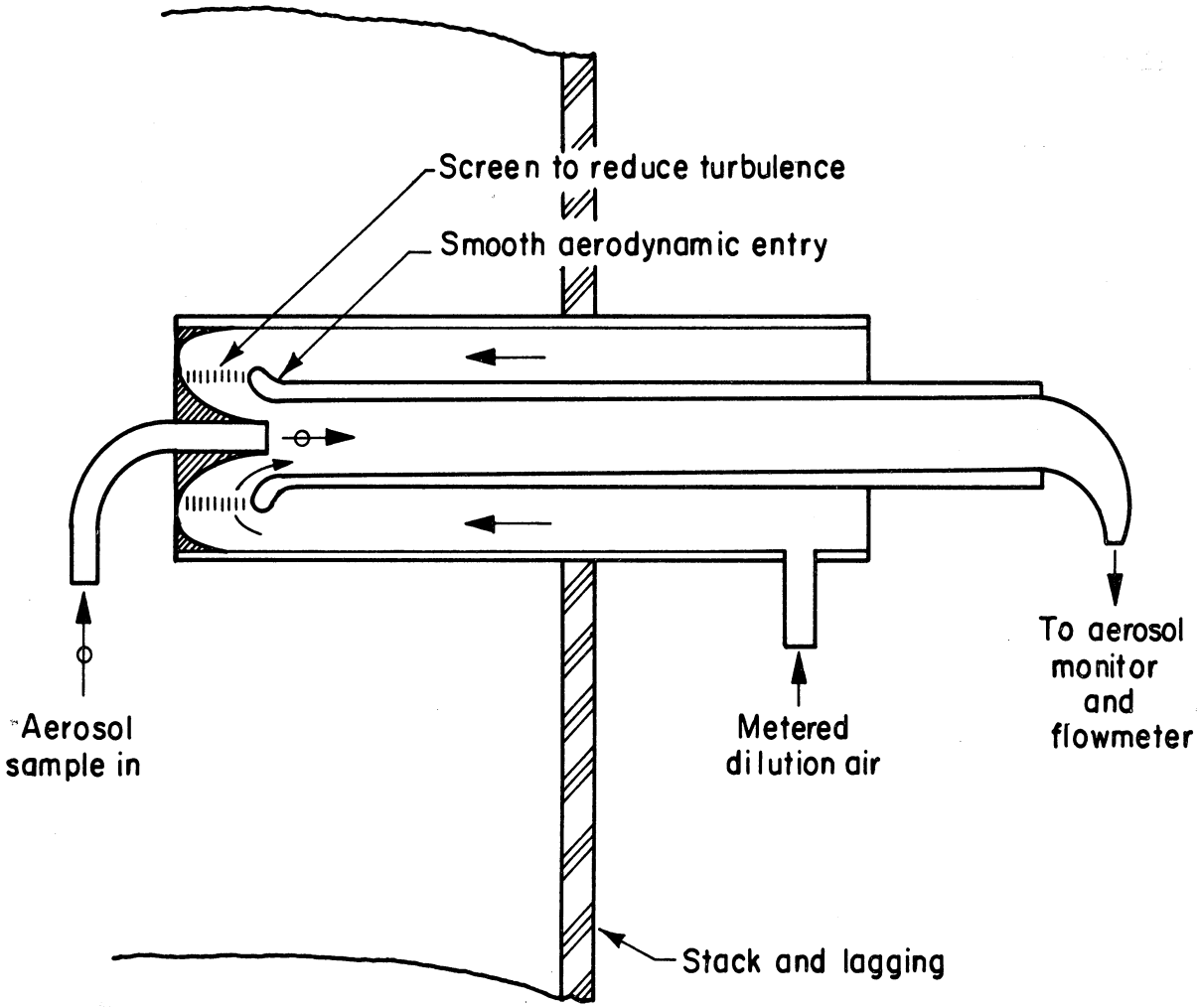

Fig. 18. Flow nozzle diluter.

B. MINIATURE TAPE SAMPLER

The design of presently available AISI Tape Stain Samplers depends upon collection of a particulate sample on a 1 in. wide Whatman or other filter paper strip. This is generally necessary because of the desire to obtain a reasonable spot for evaluation with a light source and a barrier layer photocell. In the presently conceived continuous aerosol monitor, using initial pressure drop and linear increase as a measure of the air-borne particulate concentration, the spot size could be reduced considerably. The measured pressure and its increment due to particle deposits are not a function of the filter size, but arise from filtration velocity. This implies that a quite small spot (say 1/8 in. diam) would be equally effective for this development. By reducing the spot size and increasing the velocity, a measurable pressure increment can be achieved in a substantially reduced time. This suggests the development of a miniature tape sampler of reduced size, possibly battery powered and portable. Some consideration has been given to the possible construction of this modification, and it has been discussed with interested instrument manufacturers.[8,9] It is believed that they may construct such a device for use as a tape stain sampler. The miniature sampler might have application for monitoring in sealed environments (submarines, space flight capsules, commercial aircraft in flight, etc.) and for measurement of dust concentrations in mines, mills, and general industrial atmospheres.

C. CONSTANT RESISTANCE POROUS MEDIA

The continuous aerosol monitor under development in this research depends upon the deposition of particulate matter on a porous substrate and the measure-

ment of initial and resulting pressure drop. Since the analysis of the concentration depends only upon these pressure measurements, and these are to be recorded in situ at the beginning and end of the filtration cycle, there is no particular merit in storing this deposit on a moving filter paper tape. It seems quite possible to develop a porous substrate, such as the Selas silver membrane filter, or a similar permanent type media, to be used continously in the monitor. In concept, filtration would occur in the permanent medium, and the two pressures would be recorded as an index of the concentration, and then the medium could be rotated or indexed out of the gas stream and subjected to a cleaning step. The possibilities of cleaning various kinds of metal porous media with least-generated shock waves have been explored in another AISI project, and those results may have some application to this device configuration. Other kinds of wet or dry cleaning can be considered. This concept has not been explored, as yet.

D. FILTER STUDIES

Additional studies are necessary to evaluate the response of filter pressure drop to deposition of "mixed-monodispersed" solid particles such as 1.3 μ together with 0.1 μ and 3 μ polystyrene latex. The particle resistance coefficient is theoretically independent of the particle size, and this should be established. Other studies required include response to simulant industrial particulates including iron oxide fume and pulverized fuel fly ash, and response to atmospheric dust. These can be readily conducted with apparatus described above, with use of various other aerosol generators as required.

As the prototype apparatus develops, field application evaluation would be necessary and desirable.

E. ELECTRONIC STUDIES

Based on results at this time, it appears appropriate to conduct direct feasibility studies with the Hewlett-Packard system suggested in Table IV. Their representatives have visited the laboratory and have indicated that the equipment suggested will perform satisfactorily for this application. They have further indicated it will be possible to evaluate their system prior to actually purchasing it. This seems to be the next logical step.

Other development of the sample-hold-compare circuit can proceed on the output signal from the Hewlett-Packard carrier amplifier. Other lines of electronic research include direct discussion of this application with Philbrick Researchers, Inc., for the possible development or purchase of a suitable sample-hold module.

REFERENCES

1. Billings, C. E., "Effects of Particle Accumulation in Serosol Filtration," W. M. Keck Laboratory of Environmental Health Engineering, California Institute of Technology, Sept. 1966.

2. Drinker, P. and Hatch, T., "Industrial Dust," McGraw-Hill Book Co., New York (1954).

3. Neubert, H.K.P., "Instrument Transducers," Oxford University Press, England (1963).

4. "Philbrick Application Manual--Computing Amplifiers," Philbrick Researchers, Inc., Dedham, Mass. (1966).

5. Wildhack, W. A., et al., "Continuous Absorption Hygrometry with a Pneumatic Bridge Utilizing Critical Flow," in Humidity and Moisture, Measurement and Control in Science and Industry, A. Wexler, Ed., Vol. 1, p. 552, Reinhold Publ. Corp., New York (1965).

6. Bulba, E. and Silverman, L., "A Mass Recording Stack Monitoring System for Particulates," Paper 65-141, 58th Annual Air Pollution Control Association Meeting, Toronto, Ont., Canada, June 20, 1965, p. 46.

7. Washimi, K. and Asakura, M., "Flushing Nozzle with Hydrogen Solves Sampling Problem," Chem. Eng., p. 120 (July 3, 1967).

8. Elmer E. Fleck, Research Applicance Co., Pittsburgh, Pa. May 1967, personal communication.

9. Robert A. Gussman, Singco Inc., Burlington, Mass., August 1967, personal communication.